임의의 단면 형상을 갖는 복합재료 블레이드의 첨단 구조해석 모델 개발

정 성 남*, Inderjit Chopra**

DEVELOPMENT OF A REFINED STRUCTURAL MODEL FOR COMPOSITE BLADES WITH ARBITRARY SECTION SHAPES

Sung Nam Jung*, and Inderjit Chopra†

Abstract

A general structural model, which is an extension of the Vlasov theory, is developed for the analysis of composite rotor blades with elastic couplings. A comprehensive analysis applicable to both thick- and thin-walled composite beams, which can have either open- or closed profile is formulated. The theory accounts for the effects of elastic couplings, shell wall thickness, and transverse shear deformations. A semi-complementary energy functional is used to account for the shear stress distribution in the shell wall. The bending and torsion related warpings and the shear correction factors are obtained in closed form as part of the analysis. The resulting first order shear deformation theory describes the beam kinematics in terms of the axial, flap and lag bending, flap and lag shear, torsion and torsion-warping deformations. The theory is validated against experimental results for various cross-section beams with elastic couplings.

Key Words: Composite Blades, Elastic Couplings, Wall Thickness, Transverse Shear, Warping

Introduction

During the past decade, there has been a phenomenal growth of research activities to develop methodology to analyze composite tailored rotor blades. Jung *et al.* [1] made an assessment of the current techniques of modeling composite rotor blades and identified, among others, the need for a Timoshenko type model which will take into account such features as elastic couplings, thickness of the shell wall and that will be applicable to beams having open- or closed cross-sections. The modeling of rotor blades can be formulated through either a displacement or a force method. The displacement formulation, also called the stiffness formulation has been used, among others, by Rehfield [2], Smith and Chopra [3], Chandra and Chopra [4]. This formulation is based on suitable approximations to the displacement field of the shell wall. The assumed displacement field is used to compute the strain energy and the beam stiffness relations as well as equations of motion are obtained through these energy principles. In displacement based models, the distribution of warping across the cross-section can only be applied to simple cross-sections. There is no systematic method to decide on the distribution of the warping distribution to a generic section and the choice of suitable functions. Also, in the displacement modes of these methods do not satisfy the equations of equilibrium of the shell wall and lead to overestimates of the beam stiffnesses.

In the force formulation, also called the flexibility formulation, the direct stress in the shell wall is assumed and the distribution of the shear stress and the related warpings are obtained from the equilibrium equations of the shell wall. The flexibility method provides a systematic method of choosing the warping functions. The representative ones are Mansfield and Sobey [5] and Libove [6]. While these methods give a better representation of the shear stresses, and hence a better accuracy, they have not found wide

* Assistant Professor, Faculty of Mechanical Engineering, Chonbuk National University, Chonju 561-756, Korea
† Alfred Gessow Chair Professor, University of Maryland, College Park, MD 20742, USA

application since most of the comprehensive analysis codes use the displacement method.

In the present work, a comprehensive analysis which is applicable to both thick- and thin-walled composite beams, which can have either open- or closed profile is presented. The theory accounts for the effects of elastic couplings, shell wall thickness, and transverse shear deformations. The shear related terms are obtained from the equations of equilibrium of the shell wall. The resulting first order (Timoshenko) shear deformation theory describes the beam kinematics in terms of the axial, flap and lag bending, flap and lag shear, torsion and torsion-warping deformations. The theory is validated against experimental test data and other analyses for composite beams of various cross-sections.

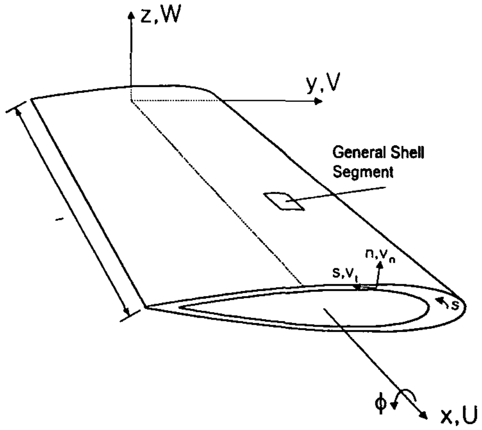

Fig. 1 Geometry and coordinate systems of a blade.

Formulation

Figure 1 shows the geometry and coordinate systems of a blade. Two systems of coordinate axes are used to describe the motion: an orthogonal Cartesian coordinate system (x, y, z) for the beam, where x is the reference axis of the beam and y and z are the transverse coordinates of the cross section; a curvilinear coordinate system (x, s, n) for the shell wall of the section, where s is a contour coordinate measured along the middle surface of the shell wall, and n is normal to this contour coordinate. The global deformations of the beam are (U, V, W) along the x, y and z axes and ϕ denotes the twist about the x-axis. The local shell deformations are (u, v_t, v_n) along the x, s, and n directions, respectively. From geometric considerations (Fig. 1) and assumption 1, the shell displacements v_n^0 and v_t^0 at the mid-plane of the wall are related to the beam displacements V, W and ϕ as:

$$
\begin{aligned}
v_t^0 &= Vy_{,s} + Wz_{,s} + r\phi \\
v_n^0 &= Vz_{,s} - Wy_{,s} - q\phi
\end{aligned}
\tag{1}
$$

where $(\ )_{,s}$ denotes differentiation with respect to s.

The constitutive relations for the shell wall of the section can be written as[14]

$$
\begin{Bmatrix} N_{xx} \\ N_{xs} \\ M_{xx} \\ M_{xs} \end{Bmatrix} = \begin{bmatrix} A'_{11} & A'_{16} & B'_{11} & B'_{16} \\ A'_{16} & A'_{66} & B'_{16} & B'_{66} \\ B'_{11} & B'_{16} & D'_{11} & D'_{16} \\ B'_{16} & B'_{66} & D'_{16} & D'_{66} \end{bmatrix} \begin{Bmatrix} \varepsilon_{xx} \\ \gamma_{xs}^c \\ \kappa_{xx} \\ \kappa_{xs} \end{Bmatrix}
\tag{2}
$$

$$N_{xn} = A_{xn}\gamma_{xn}^c$$

where, A'_{ij}, B'_{ij}, and D'_{ij} are modified laminate stiffnesses for extension, extension-bending coupling and bending, respectively. It is convenient to write the constitutive relations in a semi-inverted form as:

$$
\begin{Bmatrix} N_{xx} \\ M_{xx} \\ M_{xs} \\ \gamma_{xs}^c \end{Bmatrix} = \begin{bmatrix} C_{n\varepsilon} & C_{n\kappa} & C_{n\phi} & C_{n\tau} \\ C_{n\kappa} & C_{m\kappa} & C_{m\phi} & C_{m\tau} \\ C_{n\phi} & C_{m\phi} & C_{\phi\phi} & C_{\phi\tau} \\ -C_{n\tau} & -C_{m\tau} & -C_{\phi\tau} & C_{\gamma\tau} \end{bmatrix} \begin{Bmatrix} \varepsilon_{xx} \\ \kappa_{xx} \\ \kappa_{xs} \\ N_{xs} \end{Bmatrix}
\tag{3}
$$

$$N_{xn} = A_{xn}\gamma_{xn}^c$$

In order to assess the semi-inverted constitutive relations (5), Reissner's semi-complimentary energy function Φ_R is introduced [7]:

$$
\Phi_R = \frac{1}{2}[N_{xx}\varepsilon_{xx} + M_{xx}\kappa_{xx} + M_{xs}\kappa_{xs} + N_{xn}\gamma_{xn}^k - N_{xs}\gamma_{xs}^k]
\tag{4}
$$

The stiffness matrix relating beam forces to beam displacements is obtained by using the Reissner's semi-complimentary energy functional. The variational statement for the Reissner function gives

$$
\delta\int_0^l \oint (\Phi_R + \frac{1}{2}\gamma_{xs}^c N_{xs})dsdx = 0
\tag{5}
$$

where l is the length of the blade. Inserting the constitutive relations and the strain-displacement relation into the variation equation of (5), we obtain the relation between the generalized forces and displacements as:

$$\overline{\mathbf{F}} = \overline{\mathbf{K}}\,\overline{\mathbf{q}} \tag{6}$$

where

$$\begin{aligned} \overline{\mathbf{q}}^T &= \left[U_{,x}\ \gamma_{xy}\ \gamma_{xz}\ \phi_{,x}\ \beta_{y,x}\ \beta_{z,x}\ \phi_{,xx}\right] \\ \overline{\mathbf{F}}^T &= \left[N\ V_y\ V_z\ T_s\ M_y\ M_z\ M_\omega\right] \end{aligned} \tag{7a, b}$$

where γ_{xy} and γ_{xz} are transverse shear strains of the beam cross-section, N is axial force, V_y and V_z are transverse shear forces, M_y and M_z are bending moments about y and z directions, respectively, T_s is St. Venant Torsion, and M_ω is warping moment. Figure 2 shows the generalized beam forces acting on the blade. The (7x7) stiffness matrix $\overline{\mathbf{K}}$ in Eq. (9) represents the beam stiffness matrix at a Timoshenko level of approximation.

Results and Discussion

Numerical predictions for symmetric composite I-beams undergoing different types of loading are evaluated to validate the current approach against experimental data and other existing analytic beam results. The I-beams tested has a length of 762 mm (30 *in*) with 25.4 mm x 12.7 mm (1 *in* x 0.5 *in*) section. The beam is clamped at its root and warping restrained at both the root and loading tip. The I-section has a symmetric layup with respect to beam elastic axis and is composed of top and bottom flanges with a layup of $[(0/90)_2/(90/0)/15_2]_T$ and a web with $[0/90]_{2s}$. Figure 2 presents the bending slope distribution along the beam span for the bending-torsion coupled I-beam under a unit tip bending load using the present mixed method and the stiffness method. The stiffness approach used to calculate the stiffnesses follows Smith and Chopra [4]. The present mixed method combines both the stiffness and flexibility formulations. As can be seen in Figure 2, the current predictions with mixed formulation show better correlation with experimental data. The stiffness-based approach underpredicts bending slope of the beam. Figure 3 presents the bending-induced twist distribution along the beam span for the same beam under unit tip bending load. It is surprising that the stiffness method shows better correlation with test data than mixed method. Imposed warping restraint at the beam tip in analysis may be too restrictive and overestimates torsional stiffness of beam. Figure 4 shows the twist distribution along the beam subjected to unit tip torque. The present results of using mixed formulation show better correlation with experimental results. This fact is due to the higher accuracy in estimating bending, warping and torsion stiffnesses in the present mixed formulation.

Conclusions

A structural model has been presented for the analysis of composite blades with elastic couplings. The model includes the influence of the thickness of the wall and accounts for the non-uniform distribution of the shear strains due to bending and torsion. Beams of open and closed cross-section are modeled in a unified approach which is based on a semi-complementary energy functional and combines the displacement formulation with the flexibility formulation. The bending and torsion warpings are derived in a closed form and all the terms in the warpings are retained. Comparison of results for bending-torsion coupled I-beams shows that the present method gives results which have a good agreement with experiments.

References

1. Jung, S. N., Nagaraj, V. T. and Chopra, I., "Assessment of Composite Rotor Blade Modeling Techniques," *Journal of the American Helicopter Society*, Vol. 44, No. 3, 1999, pp.188-205.
2. Rehfield, L. W., "Design Analysis Methodology for Composite Rotor Blades," *7th DoD/NASA Conference on Fibrous Composites in Structural Design*, Denver, June 17-20, 1985.
3. Smith, E. C. and Chopra, I., "Formulation and Evaluation of an Analytical Model for Composite Box-Beams," *Journal of the American Helicopter Society*, Vol. 36, No. 3, July 1991, pp. 23-35.
4. Chandra, R. and Chopra, I., "Experimental and Theoretical Analysis of Composite I-Beams with Elastic Couplings," *AIAA Journal*, Vol. 29, No. 12, Dec. 1991, pp. 2197-2206.
5. Mansfield, E. H. and Sobey, A. J., "The Fiber Composite Helicopter Blade, Part I: Stiffness Properties, part II: Prospects for Aeroelastic Tailoring," *Aeronautical Quarterly*, Vol. 30, 1979.
6. Libove, C., "Stress and Rate of Twist in Single-Cell Thin-Walled Beams with

Anisotropic Walls," *AIAA Journal*, Vol. 26, No. 9, 1988, pp. 1107-1118.

7. Murakami, H., Reissner, E., and Yamakawa, J., "Anisotropic Beam Theories with Shear Deformation," *Journal of Applied Mechanics*, Vol. 63, No. 3, 1996, pp. 660-668.

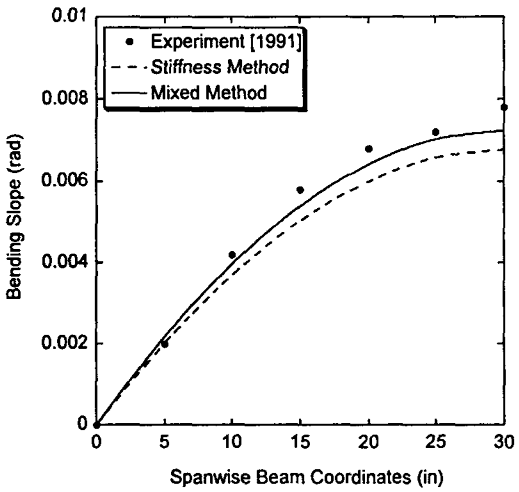

Fig. 2 Comparison of bending slope for the bending-torsion coupled I-beam under a unit tip bending load (flanges $[(0/90)_2/(90/0)/15_2]_T$, web $[(0/90)_2]_s$).

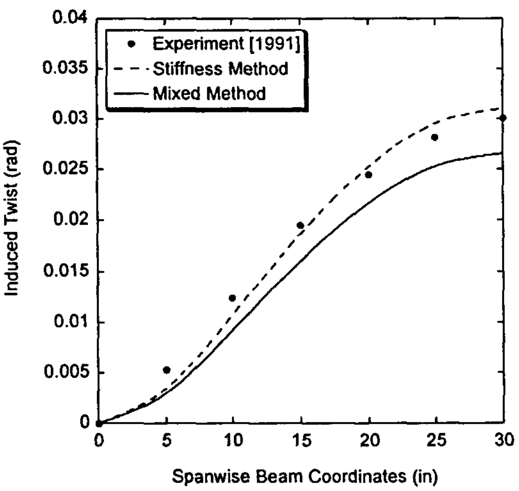

Fig. 3 Comparison of bending-induced twist distribution for the bending-torsion coupled I-beam under a unit tip bending load (flanges $[(0/90)_2/(90/0)/15_2]_T$, web $[(0/90)_2]_s$).

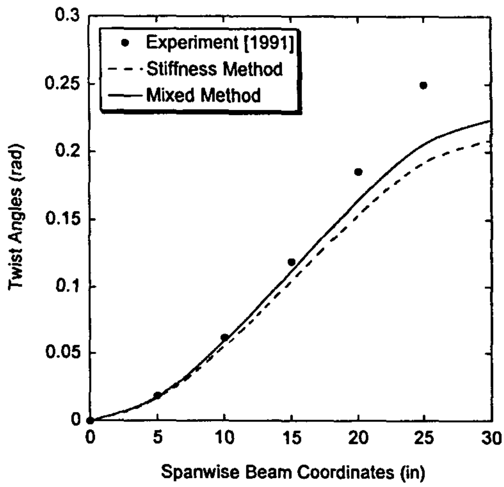

Fig. 4 Comparison of twist distribution for the bending-torsion coupled I-beam under a unit tip torque (flanges $[(0/90)_2/(90/0)/15_2]_T$, web $[(0/90)_2]_s$).